Atmos. Chem. Phys. Discuss., 12, 29099–29127, 2012
www.atmos-chem-phys-discuss.net/12/29099/2012/
doi:10.5194/acpd-12-29099-2012

Atmospheric Chemistry and Physics Discussions

Cloud-resolving modeling of aerosol indirect effects in idealized radiative-convective equilibrium with interactive and fixed sea surface temperature

M. F. Khairoutdinov[1] and C.-E. Yang[1,*]

[1]School of Marine and Atmospheric Sciences, Stony Brook University, Stony Brook, New York, USA
[*]now at: Department of Civil and Environmental Engineering, University of Tennessee, Knoxville, TN, USA

Received: 9 October 2012 – Accepted: 23 October 2012 – Published: 13 November 2012

Correspondence to: M. F. Khairoutdinov (marat.khairoutdinov@stonybrook.edu)

Published by Copernicus Publications on behalf of the European Geosciences Union.

Abstract

The study attempts to evaluate the aerosol indirect effects over tropical oceans in regions of deep convection applying a three-dimensional cloud-resolving model run over a doubly-periodic domain. The Tropics are modeled using a radiative-convective equilibrium idealization when the radiation, turbulence, cloud microphysics, and surface fluxes are explicitly represented while the effects of large-scale circulation are ignored. The aerosol effects are modeled by varying the number concentration of cloud condensation nuclei (CCN) at 1 % supersaturation, which serves as a proxy for the aerosol amount in the environment, over a wide range, starting from pristine maritime ($50\,\mathrm{cm}^{-3}$) to polluted ($1000\,\mathrm{cm}^{-3}$) conditions. No direct effects of aerosol on radiation are included. Two sets of simulations have been run to equilibrium: fixed (non-interactive) sea surface temperature (SST) and interactive SST as predicted by a simple slab-ocean model responding to the surface radiative fluxes and surface enthalpy flux. Both sets of experiments agree on the tendency to make the shortwave cloud forcing more negative and reduce the longwave cloud forcing in response to increasing CCN concentration. These, in turn, tend to cool the SST in interactive-SST case. It is interesting that the *absolute* change of the SST and most other bulk quantities depends only on *relative* change of CCN concentration; that is, same SST change can be the result of doubling CCN concentration regardless of clean or polluted conditions. It is found that the 10-fold increase of CCN concentration can cool the SST by as much as 1.5 K. This is quite comparable to 2 K warming obtained in a simulation for clean maritime conditions, but doubled CO_2 concentration. Qualitative differences between the interactive and fixed SST cases have been found in sensitivity of the hydrological cycle to the increase in CCN concentration; namely, the precipitation rate shows some tendency to increase in fixed SST case, but robust tendency to decrease in interactive SST case.

ACPD
12, 29099–29127, 2012

1 Introduction

Atmospheric aerosol plays an important role in the Earth radiative budget. The aerosol particles can directly scatter and absorb solar and terrestrial radiation. They can also indirectly influence microphysics and, hence, optical properties of clouds (Lohmann and Feichter, 2005). By convention, the aerosol indirect effects (AIEs) are subdivided into subcategories depending on their effects on cloud properties. For example, the effect of aerosols on cloud albedo is called the first indirect or Twomey effect (Twomey, 1974), the effect on precipitation efficiency (Albrecht, 1989) and cloud lifetime (Pincus and Baker, 1994) is called the second indirect effect. The current consensus reflected in the Fourth Assessment Report of the Intergovernmental Panel on Climate Change (IPCC, 2007) is that the aerosols have predominantly cooling effect on climate with the magnitude of the forcing which is quite similar to the net radiative forcing due to anthropogenic greenhouse gases. However, the magnitude of aerosol cooling remains highly uncertain, especially for the indirect effects, because of complicated nature of interactions between aerosols and clouds.

The bulk of estimates for the AIEs on global climate come from modeling studies that use general circulation models (GCMs) and cloud-resolving models (CRMs). The GCMs generally do not resolve individual clouds; therefore, virtually all the complexities of aerosol-cloud-radiation interactions have to be parameterized (e.g. Abdul-Razzak and Ghan, 2002; Nenes and Seinfeld, 2003; Liu and Penner, 2005; Hoose et al., 2010). On the other hand, many details of interactions among convection, large-scale forcing, aerosol, cloud microphysics, and radiation can be explicitly represented by CRMs (e.g. Lu and Seinfeld, 2005; Grabowski, 2006; Tao et al., 2007; van den Heever et al., 2011; Morrison and Grabowski, 2011). Recently, a GCM that uses a CRM as a superparameterization of clouds has been developed to link the explicitly simulated clouds and aerosol processes on global scale (Wang et al., 2011).

In this study, we use the CRM approach to look at the AIEs on deep tropical convection. As the Tropics occupy about half of the Earth surface, the importance of aerosol effects on the Tropics cannot be overestimated in the context of the global change problem. We use the radiative-convective equilibrium (RCE) as a proxy for the tropical atmosphere (e.g. Renno et al., 1994). In the RCE, the effects of large-scale circulation are ignored, so the convection balances the destabilization only by radiation and surface enthalpy fluxes. The RCE has been rather extensively used in the past to study processes driving hydrological cycle in the Tropics (e.g. Tompkins and Craig, 1998; Xu and Randall, 1999; Grabowski, 2006; Stephens et al., 2008). The majority of previous CRM studies of AIEs have examined the variations of tropical convection using prescribed from observations or fixed sea-surface temperature (SST; e.g. Rotstayn and Penner, 2001; Rotstayn and Lohmann, 2002; Grabowski, 2006; Morrison and Grabowski, 2011). The AIEs in the fixed-SST case can be viewed as the *fast* response of cloudy atmosphere to aerosol forcing on relatively short time scales when the SST does not have enough time to respond due to the ocean's large thermal inertia. However, the prolonged changes in aerosol forcing and associated imbalance of the energy budget at the surface will change the SST, which, in turn, will further modulate the hydrological cycle and optical properties of clouds, and, hence, should be considered as the organic part of the AIEs relevant to the climate-change problem.

The paper is organized as follows. Section 2 describes the CRM model and experimental setup. Section 3 presents the results. Section 4 provides conclusions and summary.

2 Model description and setup

2.1 Model description

The CRM used in this study is the System for Atmospheric Modeling (SAM; Khairoutdinov and Randall, 2003), version 6.8. The dynamical core solves non-hydrostatic momentum equations in anelastic approximation. The prognostic thermodynamic variable is the liquid/ice static energy, which is conserved in all moist adiabatic processes, such

ACPD
12, 29099–29127, 2012

as condensation, evaporation, freezing and melting. The subgrid-scale fluxes are modeled using eddy diffusivity/conductivity coefficients computed by the Smagorinsky–Lilly closure. The radiation scheme is a Rapid Radiative Transfer Model (RRTM; Iacono et al., 2008). The surface sensible and latent heat fluxes are computed based on Monin–Obukhov similarity. The cloud microphysics is modeled using a two-moment bulk microphysical scheme of Morrison et al. (2005), that is prognostic mixing ratio and number concentration for each of the water species, namely, cloud water, pristine cloud ice, rain, snow and graupel. In implementation for SAM, the cloud water and water vapor have been combined into a single variable, and the cloud water is diagnosed assuming no supersaturation. The source of cloud droplet number concentration is described assuming that the number of activated cloud condensation nuclei (CCN) depends on the supersaturation according to the power-law $N = C_{\mathrm{CCN}} S^k$, where C_{CCN} is prescribed concentration of CCN active at 1 % supersaturation S, and k is a constant set in this study to 0.4, which is rather typical value for the maritime conditions (Pruppacher and Klett, 1997). The change of the parameter C_{CCN} serves as a proxy for the change of aerosol burden. The CCN activation at the cloud base is parameterized using the vertical velocity and CCN spectrum parameters following Twomey (1959). Note that no direct effect of specified CCN on clear-sky radiation is included in this study.

The SST can be specified or calculated using a simple slab-ocean model with constant prescribed depth. The ocean can change its heat content through the surface radiation, enthalpy fluxes, and prescribed ocean-transport flux. The surface fluxes can vary horizontally depending on the atmospheric conditions above; however, the SST is horizontally uniform.

2.2 Experimental design

Each experiment in this study uses a three-dimensional doubly periodic domain with 128 × 128 grid cells in horizontal with 1-km grid spacing. The vertical domain has 64 grid levels with the top at 28 km and variable grid spacing, from 75 m near the surface to 500 m in the middle and upper troposphere, and coarser in stratosphere. The time

ACPD
12, 29099–29127, 2012

step is 10 s. There is a Newtonian damping layer above 20 km to minimize the effect of gravity wave reflection from the domain top. The radiative heating rates are updated every 45 time steps using time-averaged thermodynamic and cloud fields. The incoming solar radiation is prescribed as perpetual insolation of 255 W m^{-2}. The value is chosen to make the top-of-atmosphere flux imbalance be close to zero. There is no large-scale forcing, no Coriolis force, and no mean wind. To initialize convection, some random small-amplitude noise is added to temperature field near the surface.

Two sets of runs are performed as summarized by Table 1: interactive SST (prefix IA) as predicted from the slab ocean model, and SST fixed at 300 K (prefix FA). Each set contains five runs that differ only by the prescribed C_{CCN} parameter in the range from 50 cm^{-3} to 1000 cm^{-3}, representing the range of conditions, from pristine maritime to polluted continental-like. All runs use 355 ppmv for CO_2 concentration as the "present" value with the exception of IA2CO$_2$, which is identical to IA100 but with CO_2 concentration doubled. The runs FA100 and IA100 are the control representing typical clean maritime conditions. A small ocean transport flux in interactive SST simulations is set to be equal to the total surface flux imbalance computed at the end of FA100 run. This keeps the equilibrium SST in the IA100 run close to 300 K, so the statistics of the IA100 and FA100 runs are comparable. The slab-ocean depth is set to relatively deep 10 m to avoid SST oscillations. As the result of relatively large thermal inertia of such a thick slab, it takes at least 700 days for the SST in ISST runs to get sufficiently close to the equilibrium as illustrated by Fig. 1. The initial temperature, water vapor, and SST were taken from a small-domain RCE run; however, we do not show the initial profile as no sensitivity to the initial conditions is expected in 700-day long runs. The last 100 days of each run are used for sampling of the statistics.

ACPD
12, 29099–29127, 2012

3 Results

3.1 Sensitivity of sea surface temperature to CCN count

According to the first aerosol indirect effect, increasing the CCN number concentration or count would increase the concentration, but reduce the size of cloud droplets, which would increase the cloud shortwave albedo, and, hence, reduce the amount of solar radiation reaching the ocean. As the result, the equilibrium SST would decrease. This notion is well supported by Fig. 2a, which shows a rather significant decrease of SST by as much as 2 K when CCN count increases from values characteristic of pristine maritime to values characteristic of polluted continental-like conditions. It is apparent that the SST change in response to the same *absolute* change of CCN count is substantially higher for clean conditions than polluted conditions. However, the sensitivity of SST to the *relative* change of CCN count appears to be independent of the CCN count as demonstrated by Fig. 2b, which is similar to Fig. 2a, but uses logarithmic rather than linear scale for the horizontal axis. The constant slope of the SST dependence in Fig. 2b means that doubling the CCN count from 500 to 1000 cm^{-3} would have the same effect on SST as doubling from 50 to 100 cm^{-3}. Similar behavior is found for most other bulk quantities; therefore, as in some other studies of the AIEs, it is natural to define a *relative susceptibility* S_A as the rate of change of some quantity A with respect to change of logarithm of CCM count:

$$S_A = \partial A / \partial \log(C_{\mathrm{CCN}}) \tag{1}$$

For the SST, the relative susceptibility is estimated to be −1.5 K. In other words, in our idealized tropics, it would take one order of magnitude increase of CCN count to cool the SST by 1.5 K. It is worth noting that it is comparable in magnitude to about 2 K warming in our double-CO_2 experiment (see Fig. 1). Thus, in our RCE experiments, increasing the CCN count may effectively mitigate or mask most of the surface warming associate with the doubling of CO_2.

ACPD
12, 29099–29127, 2012

Title Page
Abstract | Introduction
Conclusions | References
Tables | Figures
◀◀ | ▶▶
◀ | ▶
Back | Close
Full Screen / Esc
Printer-friendly Version
Interactive Discussion

3.2 Radiative fluxes

The top-of-atmosphere (TOA) shortwave and longwave radiation fluxes are shown by Fig. 3 and listed by Table 2. The effect of clouds on radiation fluxes is usually described in terms of cloud radiative forcing, which is the difference between TOA clear-sky and cloudy-sky fluxes. The response of the shortwave cloud forcing (SWCF), which is typically negative, to the increase of CCN count is similar between interactive and prescribed SST cases, and consistent with the general consensus on the first AIE (Fig. 3a), that is the increase of CCN count makes SWCF more negative as clouds become brighter because of higher droplet concentrations, and, hence, smaller droplets. The relative susceptibility of SWCF is estimated to be in the range from $-0.95\,\mathrm{W\,m^{-2}}$ in FSST cases to $-1.36\,\mathrm{W\,m^{-2}}$ in ISST cases. Virtually all of the SWCF change is from the change in absorbed shortwave radiation due to clouds, because the clear-sky solar absorbed radiation is not sensitive to changes in CCN (see Table 2).

In contrast to solar TOA fluxes, the net longwave radiative flux (LWNT; Table 2) or outgoing longwave radiation (OLR; Fig. 3d) shows qualitatively different response between ISST and FSST cases. The changes in SST and the cloud water seem to be the key factors that may explain these qualitative differences. In ISST case, the OLR decreases as SST cools in response to increasing CCN count, mainly due to decrease of the clear-sky OLR (Fig. 3e). On the other hand, in FSST case, the clear-sky OLR changes are expectedly small, so that the effect of decreasing cloud fraction of anvils and corresponding ice water path (see Table 2) dominates the increase of OLR as more longwave radiation from the surface is able to reach the TOA. Despite these qualitative differences in OLR sensitivity, the sensitivity of the longwave cloud radiative forcing (LWCF; Fig. 3b), which is typically positive, to the increase of the CCN concentration is qualitatively similar between ISST and FSST cases, that is, they both indicate the reduction of the greenhouse effect associated with clouds. Quantitatively though, the relative susceptibility of the LWCF in FSST cases is about twice as high as in the ISST cases, $-2.58\,\mathrm{W\,m^{-2}}$ vs. $-1.25\,\mathrm{W\,m^{-2}}$.

ACPD
12, 29099–29127, 2012

The relative susceptibility of the total cloud radiative forcing (SWCF + LWCF; Fig. 3c) is rather similar in FSST and ISST cases, −3.53 vs. −2.61 $\mathrm{W\,m^{-2}}$, respectively. Both estimates are quantitatively consistent with the results of Menon et al. (2002), which concluded that AIE is responsible for a 1.2–3.0 $\mathrm{W\,m^{-2}}$ reduction of radiation over ocean, and the results of Ghan et al. (2001), which estimated the negative radiative forcing due to AIEs of about 1.5–3.0 $\mathrm{W\,m^{-2}}$.

In RCE, the net TOA radiative flux and the total surface flux (sum of latent, sensible and net radiation fluxes) should be equal; thus the TOA imbalance (Fig. 3f) implies the tendency of the SST to change. As expected, in ISST runs, the imbalance is generally small, less than 0.5 $\mathrm{W\,m^{-2}}$. It would take much longer runs to make the imbalance smaller, which would probably not change the results so that to warrant the additional computational expense. However, in FSST runs, there is a clear strong tendency for the negative imbalance to increase with increasing CCN concentration. Such a relatively large imbalance would lead to rapid cooling of the SST if it was allowed to adjust.

3.3 Hydrological cycle and cloud statistics

As expected, the column integrated water vapor, or precipitable water, is virtually insensitive to CCN changes in FSST runs; however, it is very sensitive to CCN changes in ISST case, as illustrated by Fig. 4a. The relative susceptibility of the precipitable water in the latter case is −5.2 mm or 13 % relative to the control case, which is rather similar to the sensitivity given by the Clasius–Clapeyron relation in response to the reduction of SST. The precipitation in ISST cases decreases in response to drying atmosphere, with the estimated relative susceptibility of −0.17 $\mathrm{mm\,day^{-1}}$ or about 5 % relative to the control case. The much slower rate of the precipitation change relative to the precipitable water change in response to the SST variation is explained by the notion that the equilibrium precipitation is mostly determined by the net radiative cooling, which does not change as fast as the water vapor mixing ratio (see, for example, Held and Soden, 2006). Despite constant precipitable water in FSST cases, the precipitation rate tends to increase with increasing CCN count, with estimated relative susceptibility of

ACPD
12, 29099–29127, 2012

0.06 mm day^{-1} or about 2 % relative to the control case. Such a relatively minor change in precipitation rate is consistent with other studies (e.g. Rotstayn and Penner, 2001; van den Heever et al., 2011; Morrison and Grabowski, 2011). The increase is the response to modest increase of radiative cooling as indicated by the increase of OLR (see Fig. 3d). It has recently been argued (e.g. Rosenfeld et al., 2008) that in mixed clouds, the suppression of warm precipitation as the result of increasing CCN count would cause the additional freezing of liquid water, which would, in turn, lead to increase of cold-phase precipitation, so-called "rain invigoration" effect. Although the physics of the proposed invigoration effect is plausible on short time scales, in our RCE simulations, the radiative constrains on hydrological cycle over longer time scales clearly keep the relative increase of precipitation over constant SST relatively small.

The changes in cloud fraction (Table 2) have been estimated using the ISCCP (International Satellite Cloud Climatology Project; Rossow and Schiffer, 1999) Simulator (Klein and Jacob, 1999). The Simulator samples the clouds to mimic cloud fraction retrieval from a satellite, that is the way most relevant to the estimates of the TOA radiative fluxes. For example, low-level clouds underneath a thick anvil cloud would not be seen by a satellite in both shortwave and longwave parts of the spectrum, and, thus, would not contribute to the estimate of the low-level cloud fraction. Sampled clouds are subdivided into three categories according to cloud-top pressure: low, middle and high. In our RCE simulations, most of the 57 % of the total cloud fraction as seen by the ISCCP Simulator is due to high-level clouds. From Table 2, it follows that as CCN count increases, the fractions of high-level (HCLD) and low-level (LCLD) clouds tend to decrease, while the fraction of mid-level (MCLD) clouds tends to increase. However, the absolute changes in cloud fraction are rather small and may not be statistically significant.

In contrast to cloud fraction, the changes in column integrals, or paths, of all five prognostic water-content variables (cloud liquid water, cloud ice, rainwater, snow, and graupel) in response to increasing CCN concentration are robust and qualitatively similar between ISST and FSST cases as shown by Fig. 5. Higher CCN counts and, hence, smaller cloud droplets result in suppression of warm rain production and, consequently, in increase of liquid water path (Fig. 5a). Corresponding relative susceptibility in FSST case is about twice as high as in ISST case (4.6 vs 2.3 $g m^{-2}$, or 14 % vs. 7 % with respect to the control). Higher cloud liquid water content means more water transported above the freezing level, which means more water is available for the cold-phase precipitation processes. This is confirmed by the monotonic increase of snow (Fig. 5d) and graupel (Fig. 5e) water paths, which, in turn, results in lower cloud ice path (Fig. 5b).

The vertical profiles of the relative change of horizontally averaged cloud and precipitating water-content variables with respect to the control runs are shown in Fig. 6. In FSST cases, the changes in CCN count do not have notable effect on clouds below 2 km, simply because of relatively small liquid cloud content and, consequently, insignificant warm rain production. In ISST cases, though, there is a considerable decrease of cloud water below 2 km, which could be explained by the effect of entrainment of dryer environment on the liquid water content at cooler SST. In the main warm-rain production region above 2 km, the microphysical effects of CCN increase are similar in FSST and ISST cases, that is to suppress rain production and, consequently, increase cloud liquid water. The reduction of the rainwater content for the same CCN count is larger in ISST cases because of the overall reduction of available water vapor in response to cooler SSTs. However, in the mixed-phase cloud regions, below 9 km, the amount of the frozen precipitation for the same CCN count is higher in ISST cases despite the cooler SSTs, which can be explained by the lower height of the freezing level and, hence, overall increase of the depth of the mixed-phase cloud region, where most of the precipitation production occurs. The cooler troposphere temperature in ISST cases can also explain the local increase of cloud ice around 8-km height level as the result of heterogeneous freezing and further increase of cloud ice due to the Bergeron–Findeisen process, which also contributes to the increase of frozen precipitation. The effect of lower availability of water vapor in ISST cases becomes apparent above 9 km in the anvil region, where the reduced amount of cloud ice results in consequent reduction of snow and graupel.

ACPD
12, 29099–29127, 2012

Despite qualitative and quantitative similarity in response of the hydrometeors to CCN changes in ISST and FSST cases, the responses of precipitation flux are rather different, as shown in Fig. 7. Note that precipitation flux for a given hydrometeor depends non-linearly on water content and number concentration. The convergence rates for the moments in two-moment bulk microphysics scheme used in this study are also complicated and nonlinear functions of the moments themselves as well as of other variables such as temperature and humidity. Therefore, it is rather difficult to untangle all the details of precipitation flux changes in response to changes in CCN count. However, qualitatively, the difference between ISST and FSST cases is mostly due to thermodynamic response of convection to changes in water vapor amount due to SST changes and also changes in the efficiency of cloud liquid water convergence to rain. In FSST cases, the reduction of convergence efficiency increases the amount of water available for the cold-phase precipitation processes, which results in overall increase of precipitation flux (Fig. 7b). On the other hand, in ISST cases, a decrease of water vapor in response to SST cooling becomes as powerful a factor in determining the precipitation rate as the changes in cloud microphysics. Overall, there is a robust reduction of precipitation flux at all levels in ISSP cases relative to FSST cases for the same CCN count (Fig. 7a).

4 Summary

This study examines the aerosol indirect effects (AIEs) in idealized tropical atmosphere using a three-dimensional cloud-resolving model with a two-moment bulk microphysics and interactive radiation. All runs use a three-dimensional doubly periodic 128 × 128 × 28 km domain with the horizontal grid spacing of 1 km. On long temporal and spatial scales, the tropical convection can be viewed as the equilibrium response to the large-scale destabilization by radiation, surface enthalpy fluxes and large-scale circulation. We use a radiative-convective equilibrium as idealization of the tropical atmosphere, in which the radiation and surface fluxes are interactively computed, but the

Discussion Paper | Discussion Paper | Discussion Paper | Discussion Paper |
ACPD
12, 29099–29127, 2012
Cloud-resolving modeling of aerosol indirect effects
M. F. Khairoutdinov and C.-E. Yang

effects of large-scale circulation are ignored. The novel feature of this study is the use of interactive SST (ISST) as predicted by a simple slab ocean model. This approach is much more computationally expensive than a commonly used fixed-SST (FSST) approach, because it takes relatively long integration time (hundreds of days) to approach the equilibrium.

The aerosol effects on clouds are modeled by prescribing the activation spectrum of cloud condensation nuclei (CCN). The CCN count is defined as CCN concentration at 1 % supersaturation. For each prescribed or prognostic SST case, five runs with increasing CCN count have been performed. The CCN count has been changed in a rather wide range, from values that are typical for pristine maritime conditions ($50\,\mathrm{cm}^{-3}$) to values that are typical for maritime polluted or even continental-like conditions ($1000\,\mathrm{cm}^{-3}$). Note that no direct effect of CCN on radiation has been included.

As expected, the equilibrium SST decreases in response to increasing CCN count. It is found that the SST sensitivity to the *absolute* change in CCN is substantially higher in clean than polluted conditions. However, the SST response to the *relative* change in CCN is independent of CCN conditions. For example, doubling CCN count in clean maritime conditions causes the same drop in SST as doubling CCN count in polluted conditions. A similar behavior is found for other bulk quantities, such as top-of-atmosphere radiative fluxes, precipitation rate, precipitable water, among others. As a quantitative measure of sensitivity of some given quantity to relative change in CCN count, we use the relative susceptibility defined as the rate of change of that quantity in response to the change of logarithm of CCN concentration. For example, the relative susceptibility of the SST is found to be $-1.5\,\mathrm{K}$, which means that it would take one order of magnitude increase of CCN count to cool the SST by that amount. Note that this cooling is quite comparable to the magnitude of the SST warming in the run with clean maritime conditions, but with doubled CO_2 concentration.

The shortwave cloud forcing (SWCF) due to CCN increase is found to become more negative in both FSST and ISST runs, which is consistent with the first indirect aerosol effect or so-called cloud-albedo effect. The relative susceptibility of the SWCF is found

ACPD
12, 29099–29127, 2012

to be $-0.95\,\mathrm{W\,m^{-2}}$ and $-1.36\,\mathrm{W\,m^{-2}}$, respectively, with virtually no changes in clear-sky shortwave radiation. The magnitude of cooling in the shortwave part of the spectrum is matched or even exceeded by the reduction in the longwave cloud radiative forcing (LWCF); however, the mechanism for the effect is different between FSST and ISST cases. In FSST case, the reduction is dominated by the decrease of the greenhouse effect of clouds, while in ISST case, it is mostly due to decrease of the clear-sky greenhouse effect caused by reduction of precipitable water in response to cooler SSTs. The magnitude of relative susceptibility of LWCF in FSST case is found to be twice as large as in ISST case, $-2.58\,\mathrm{W\,m^{-2}}$ vs. $-1.25\,\mathrm{W\,m^{-2}}$. Relative susceptibility of the net cloud radiative forcing (SWCF + LWCF) is found to be $-3.53\,\mathrm{W\,m^{-2}}$ in FSST case and $-2.61\,\mathrm{W\,m^{-2}}$ in ISST case.

There are pronounced differences between FSST and ISST cases in simulated hydrological cycle. In FSST cases, the precipitable water is virtually insensitive to changes in CCN as it mostly determined by the fixed SST, while in ISST cases, the precipitable water closely follows the SST trend, as dictated by the Clasius–Clapeyron relation. The relative susceptibility of precipitable water is found to be -5.2 mm or 13 % decrease per order of magnitude increase of CCN count. It is interesting that the sensitivity of precipitation rate is found to be of different sign between FSST and ISST cases. In FSST case, the precipitation rate tends to increase slightly in response to increasing CCN count with susceptibility of $0.06\,\mathrm{mm\,day^{-1}}$ or about 2 %. However, in ISST case, the precipitation decreases following the drying of atmosphere due to cooler SST with the relative susceptibility of $-0.17\,\mathrm{mm\,day^{-1}}$ or -5 %.

The response of the column integrals of cloud condensate and hydrometeors is found to be qualitatively similar between FSST and ISST cases. The liquid water path (LWP) tends to increase with increasing CCN count as the result of suppression of warm rain production. The relative susceptibility of LWP is $4.6\,\mathrm{g\,m^{-2}}$ (14 %) in FSST case vs. $2.3\,\mathrm{g\,m^{-2}}$ (7 %) in ISST case. As liquid water content increases, more water becomes available for cold-phase precipitation processes above the freezing level. As the result, the snow and graupel water paths increase at the expense of the cloud ice water path.

ACPD
12, 29099–29127, 2012

The results of this study demonstrate the importance of including the SST feedback when estimating the AIEs. The RCE over the fixed SST develops rather significant negative surface energy imbalance when conditions change from clean to polluted. Such an imbalance, given sufficient time, would force the SSTs to cool, which would affect the thermodynamic state and radiation field and, consequently, the convection itself. Arguably, such a *slow* response of simulated tropics to prolonged aerosol forcing may be more relevant to the climate-change problem or so-called "geo-engineering" mitigation strategy. The AIEs estimated in a fixed-SST framework may represent a *fast* response of tropical convection to changes in aerosol forcing on relatively short time scales of a few days or, perhaps, as long as a few weeks, during which the SST stays relatively unchanged due to the ocean's large heat inertia. The fast and slow feedbacks of tropical convection to aerosol forcing can be qualitatively different as we saw in the case of precipitation response.

In conclusion, we have to emphasize that the results reported here have been obtained using an idealized framework of radiative-convective equilibrium with no feedback to large-scale circulation, which can also affect the response of tropical convection to AIEs. We also do not know how sensitive our results are to the choice of microphysics scheme with quite simplified treatment of CCN as constant background with no sources and sinks. Due to relatively high computational cost of the RCE simulations over interactive SST, no test of sensitivity of our results to the grid spacing and domain size has been done. The simulations of small shallow clouds can particularly be sensitive to the grid spacing. Relatively small domain size used in this study could also prevent possible changes in convective organization in response to modification of cloud microphysics and radiation caused by changes in aerosols. These are just a few caveats among many others that need to be addressed in the future numerical studies of indirect aerosol effects.

Acknowledgements. This research was supported by the National Oceanic and Atmospheric Administration (NOAA) grant NA08OAR4310544 to Stony Brook University. M. K. was also supported by the NSF Science and Technology Center for Multiscale Modeling of Atmospheric

ACPD

12, 29099–29127, 2012

Cloud-resolving modeling of aerosol indirect effects

M. F. Khairoutdinov and C.-E. Yang

Title Page
Abstract | Introduction
Conclusions | References
Tables | Figures
◂ | ▸
Back | Close
Full Screen / Esc
Printer-friendly Version
Interactive Discussion

Processes (CMMAP), managed by Colorado State University under cooperative agreement ATM-0425247. Computing resources were provided by the New York Center for Computational Science, which is a joint venture between Stony Brook University and Brookhaven National Laboratory.

References

Abdul-Razzak, H. and Ghan, S. J.: A parameterization of aerosol activation: 3. Sectional representation, J. Geophys. Res., 107, 4026, doi:10.1029/2001JD000483, 2002.

Albrecht, B.: Aerosols, cloud microphysics, and fractional cloudiness, Science, 245, 1227–1230, 1989.

Ghan, S. J., Easter, R. C., Chapman, E. G., Abdul-Razzak, H., Zhang, Y., Leung, L. R., Laulainen, N. S., Saylor, R. D., and Zaveri, R. A.: A physically based estimate of radiative forcing by anthropogenic sulfate aerosol, J. Geophys. Res., 106, 5279–5293, doi:10.1029/2000JD900503, 2001.

Grabowski, W. W.: Indirect impact of atmospheric aerosols in idealized simulations of convective–radiative quasi equilibrium, J. Climate, 19, 4664–4682, 2006.

Held, I. M. and Soden, B. J.: Robust responses of the hydrological cycle to global warming, J. Climate, 19, 5686–5699, 2006.

Hoose, C., Kristjánsson, J. E., Chen, J.-P., and Hazra, A.: A classical-theory-based parameterization of heterogeneous ice nucleation by mineral dust, soot, and biological particles in a global climate model, J. Atmos. Sci., 67, 2483–2503, doi:10.1175/2010JAS3425.1, 2010.

Iacono, M. J., Delamere, J., Mlawer, E., Shephard, M., Clough, S., and Collins, W.: Radiative forcing by long-lived greenhouse gases: calculations with the AER radiative transfer models, J. Geophys. Res., 113, D13103, doi:10.1029/2008JD009944, 2008.

IPCC: Climate Change: The Physical Science Basis, Contribution of Working Group I to the Fourth Assessment Report of the Intergovernmental Panel on Climate Change, edited by: Solomon, S., Qin, D., Manning, M., Chen, Z., Marquis, M., Averyt, K. B., Tignor, M., and Miller, H. L., Cambridge University Press, Cambridge, UK and New York, NY, USA, 2007.

Khairoutdinov, M. F. and Randall, D. A.: Cloud-resolving modeling of the ARM summer 1997 IOP: model formulation, results, uncertainties and sensitivities, J. Atmos. Sci., 60, 607–625, 2003.

Klein, S. and Jacob, C.: Validation and sensitivities of frontal clouds simulated by the ECMWF model, Mon. Weather Rev., 127, 2514–2531, 1999.
Liu, X. and Penner, J. E.: Ice nucleation parameterization for global models, Meteorol. Z., 14, 499–514, doi:10.1127/0941-2948/2005/0059, 2005.
Lu, M.-L. and Seinfeld, J. H.: Study of the aerosol indirect effect by large-eddy simulation of marine stratocumulus, J. Atmos. Sci., 62, 3909–3932, doi:10.1175/JAS3584.1, 2005.
Lohmann, U. and Feichter, J.: Global indirect aerosol effects: a review, Atmos. Chem. Phys., 5, 715–737, doi:10.5194/acp-5-715-2005, 2005.
Menon, S., Del Genio, A. D., Koch, D., and Tselioudis, G.: GCM Simulations of the aerosol indirect effect: sensitivity to cloud parameterization and aerosol burden, J. Atmos. Sci., 59, 692–713, 2002.
Morrison, H. and Grabowski, W. W.: Cloud-system resolving model simulations of aerosol indirect effects on tropical deep convection and its thermodynamic environment, Atmos. Chem. Phys., 11, 10503–10523, doi:10.5194/acp-11-10503-2011, 2011.
Morrison, H., Curry, J. A., and Khvorostyanov, V. I.: A new double-moment microphysics parameterization for application in cloud and climate models, Part I: Description, J. Atmos. Sci., 62, 1665–1677, 2005.
Nenes, A. and Seinfeld, J. H.: Parameterization of cloud droplet formation in global climate models, J. Geophys. Res., 108, 4415, doi:10.1029/2002JD002911, 2003.
Pincus, R. and Baker, M. B.: Effect of precipitation on the albedo susceptibility of clouds in the marine boundary layer, Nature, 372, 250–252, doi:10.1038/372250a0, 1994.
Pruppacher H. R. and Klett, J. D.: Microphysics of Clouds and Precipitation, Kluwer Academic Publishers, USA, 1997.
Rennó, N. O., Emanuel, K. A., and Stone, P. H.: Radiative-convective model with an explicit hydrological cycle, Part I: Formulation and sensitivity to model parameters, J. Geophys. Res., 99, 14429–14441, 1994.
Rosenfeld, D., Lohmann, U., Raga, G. B., O'Dowd, C. D., Kulmala, M., Fuzzi, S., Reissell, A., and Andreae, M.: Flood or drought: how do aerosols affect precipitation?, Science, 321, 1309–1313, 2008.
Rossow, W. B. and Schiffer, R. A.: Advances in understanding clouds from ISCCP, B. Am. Meteorol. Soc., 80, 2261–2288, 1999.
Rotstayn, L. D. and Lohmann, U.: Tropical rainfall trends and the indirect aerosol effect, J. Climate, 15, 2103–2116, 2002.

ACPD
12, 29099–29127, 2012

Cloud-resolving modeling of aerosol indirect effects

M. F. Khairoutdinov and C.-E. Yang

Rotstayn, L. D. and Penner, J. E.: Indirect aerosol forcing, quasi forcing, and climate response, J. Climate, 14, 2960–2975, 2001.

Stephens, G. L., van den Heever, S., and Pakula, L.: Radiative–convective feedbacks in idealized states of radiative–convective equilibrium. J. Atmos. Sci., 65, 3899–3916, 2008.

Tao, W.-K., Li, X., Khain, A., Matsui, T., Lang, S., and Simpson, J.: Role of atmospheric aerosol concentration on deep convective precipitation: cloud-resolving model simulations, J. Geophys. Res., 112, D24S18, doi:10.1029/2007JD008728, 2007.

Tompkins, A. M., and Craig, G. C.: Radiative-convective equilibrium in a three-dimensional cloud ensemble model, Q. J. Roy. Meteor. Soc., 124, 2073–2097, 1998.

Twomey, S.: The nuclei of natural cloud formation. Part II: The supersaturation in natural clouds and the variation of cloud droplet concentrations, Pure Appl. Geophys., 43, 243–249, 1959.

Twomey, S.: Pollution and the planetary albedo, Atmos. Environ., 8, 1251–1256, 1974.

van den Heever, S. C., Stephens, G. L., and Wood, N. B.: Aerosol indirect effects on tropical convection characteristics under conditions of radiative–convective equilibrium, J. Atmos. Sci., 68, 699–718. doi:10.1175/2010JAS3603.1, 2011.

Wang, M., Ghan, S., Easter, R., Ovchinnikov, M., Liu, X., Kassianov, E., Qian, Y., Gustafson Jr., W. I., Larson, V. E., Schanen, D. P., Khairoutdinov, M., and Morrison, H.: The multi-scale aerosol-climate model PNNL-MMF: model description and evaluation, Geosci. Model Dev., 4, 137–168, doi:10.5194/gmd-4-137-2011, 2011.

Xu, K.-M. and Randall, D. A.: A sensitivity study of radiative–convective equilibrium in the tropics with a convection-resolving model, J. Atmos. Sci., 56, 3385–3399, 1999.

ACPD

12, 29099–29127, 2012

Cloud-resolving modeling of aerosol indirect effects

M. F. Khairoutdinov and C.-E. Yang

Table 1. List of simulations.

Interactive SST		Fixed SST	
Case	C_{CCN} (cm^{-3})	Case	C_{CCN} (cm^{-3})
IA50	50	FA50	50
IA100	100	FA100	100
IA200	200	FA200	200
IA500	500	FA500	500
IA1000	1000	FA1000	1000
IA2CO$_2$	100		

ACPD
12, 29099–29127, 2012

Table 2. Simulation results (see Table 3 for the list of abbreviations).

Case	SST (K)	PW (mm)	PREC ($\mathrm{mm\,day^{-1}}$)	SHF ($\mathrm{W\,m^{-2}}$)	LHF ($\mathrm{W\,m^{-2}}$)	
IA50	300.52	40.82	3.17	10.25	92.30	
IA100	300.09	39.20	3.12	10.33	90.82	
IA200	299.60	37.50	3.07	10.45	89.27	
IA500	298.95	35.43	3.00	10.56	87.17	
IA1000	298.55	34.27	2.95	10.61	85.81	
IA2CO_2	302.01	47.05	3.37	9.77	97.94	
FA50	300.00	38.92	3.10	10.32	89.96	
FA100	300.00	38.91	3.11	10.33	90.36	
FA200	300.00	38.91	3.13	10.40	90.91	
FA500	300.00	38.90	3.16	10.52	91.72	
FA1000	300.00	38.98	3.17	10.57	92.08	
Case	LWNT ($\mathrm{W\,m^{-2}}$)	LWNTC ($\mathrm{W\,m^{-2}}$)	SWNT ($\mathrm{W\,m^{-2}}$)	SWNTC ($\mathrm{W\,m^{-2}}$)	LWCF ($\mathrm{W\,m^{-2}}$)	SWCF ($\mathrm{W\,m^{-2}}$)
IA50	222.08	264.28	222.57	240.91	42.20	−18.34
IA100	221.87	263.73	222.21	240.89	41.86	−18.68
IA200	221.74	263.03	221.92	240.88	41.29	−18.96
IA500	221.29	262.10	221.27	240.85	40.81	−19.58
IA1000	220.77	261.52	220.68	240.84	40.75	−20.16
IA2CO_2	222.18	261.23	222.87	240.96	39.05	−18.09
FA50	221.16	263.68	222.50	240.89	42.52	−18.39
FA100	221.68	263.55	222.20	240.89	41.86	−18.69
FA200	222.41	263.51	221.94	240.89	41.10	−18.95
FA500	223.57	263.41	221.59	240.89	39.84	−19.30
FA1000	223.94	263.32	221.21	240.89	39.38	−19.68

ACPD
12, 29099–29127, 2012

Table 2. Continued.

Case	CWP ($g\,m^{-2}$)	IWP ($g\,m^{-2}$)	RWP ($g\,m^{-2}$)	SWP ($g\,m^{-2}$)	GWP ($g\,m^{-2}$)
IA50	31.44	17.13	34.62	24.13	42.34
IA100	32.13	16.88	31.47	26.82	44.59
IA200	32.86	16.42	28.79	30.61	46.94
IA500	33.62	16.02	25.54	35.91	49.25
IA1000	34.52	15.82	23.84	39.00	50.90
IA2CO_2	33.66	16.38	34.86	24.39	45.81
FA50	30.57	17.41	33.45	24.29	42.62
FA100	32.04	16.93	31.31	26.90	44.56
FA200	33.42	16.35	29.70	29.53	46.90
FA500	35.21	15.74	28.28	32.97	50.24
FA1000	36.71	15.32	27.59	35.24	52.42

Case	LCLD (%)	MCLD (%)	HCLD (%)	TCLD (%)
IA50	3.04	2.61	51.86	57.51
IA100	2.88	2.67	51.81	57.36
IA200	2.81	2.77	51.45	57.02
IA500	2.76	2.89	50.62	56.27
IA1000	2.73	3.14	51.36	57.22
IA2CO_2	3.20	2.53	49.92	55.64
FA50	2.93	2.55	51.71	57.20
FA100	2.87	2.66	51.81	57.34
FA200	2.85	2.79	51.44	57.08
FA500	2.85	2.88	50.21	55.94
FA1000	2.82	3.02	50.19	56.04

ACPD
12, 29099–29127, 2012

Cloud-resolving modeling of aerosol indirect effects

M. F. Khairoutdinov and C.-E. Yang

Table 3. Abbreviations.

Parameter	Explanation
CWP	Cloud water path
HCLD	high-level cloud fraction as estimated by the ISCCP Cloud Simulator
IWP	Ice water path
GWP	Graupel water path
LCLD	low-level cloud fraction as estimated by the ISCCP Cloud Simulator
LHF	Latent heat flux
LWCF	longwave cloud radiative forcing
LWNT	net longwave radiation flux at the top of the atmosphere
LWNTC	net longwave radiation flux at the top of the atmosphere at clear sky
MCLD	mid-level cloud fraction as estimated by the ISCCP Cloud Simulator
PREC	surface precipitation
PW	precipitable water
RWP	rainwater water path
SHF	sensible heat flux
SST	sea surface temperature
SWCF	shortwave cloud radiative forcing
SWNT	net shortwave radiation flux at the top of the atmosphere
SWNTC	net shortwave radiation flux at the top of the atmosphere at clear sky
SWP	snow water path
TCLD	total cloud fraction as estimated by the ISCCP Cloud Simulator

ACPD
12, 29099–29127, 2012

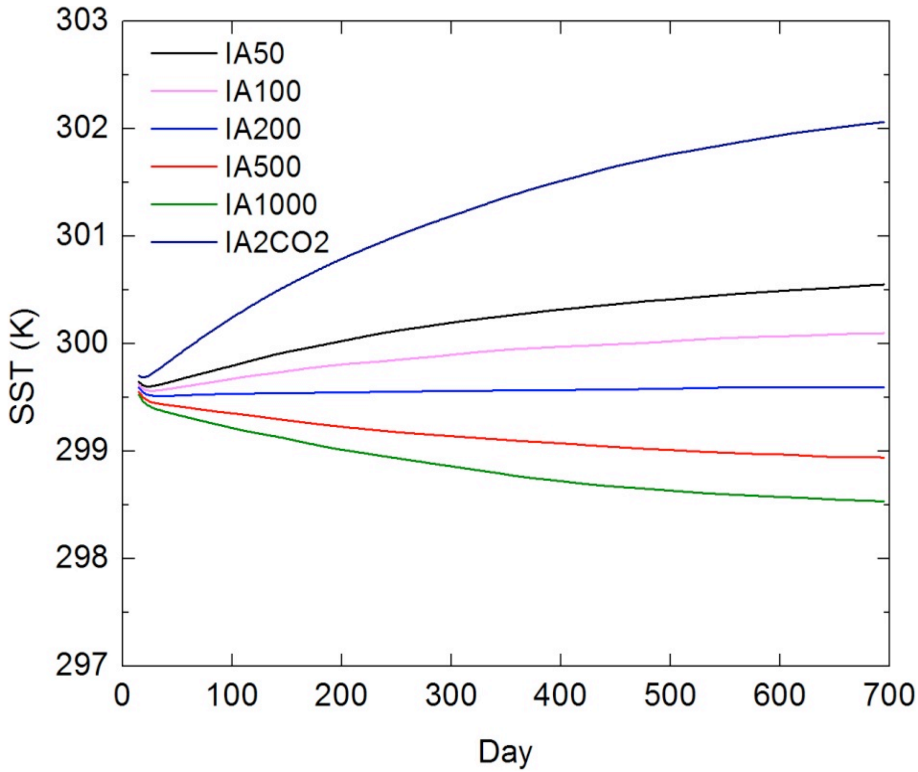

Fig. 1. Time evolution of the SST in interactive-SST runs.

ACPD
12, 29099–29127, 2012

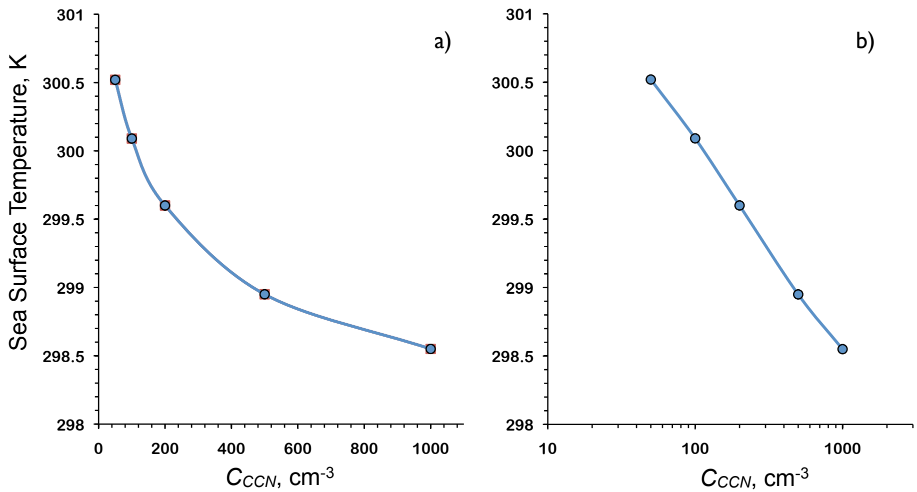

Fig. 2. Dependence of near-equilibrium SST on the CCN number concentration at 1 % supersaturation plotted as **(a)** linear and **(b)** logarithmic scales.

ACPD
12, 29099–29127, 2012

Cloud-resolving modeling of aerosol indirect effects

M. F. Khairoutdinov and C.-E. Yang

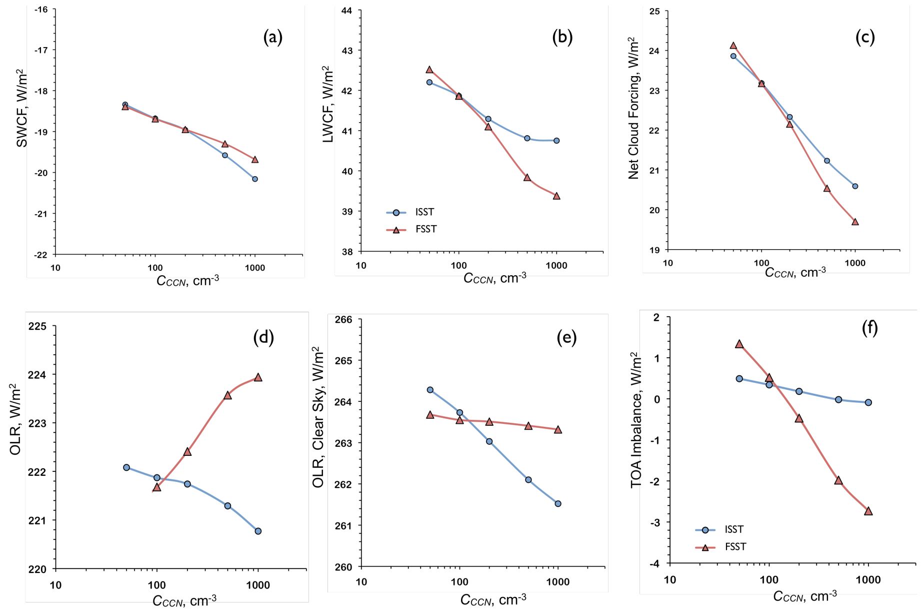

Fig. 3. Dependence of **(a)** SWCF, **(b)** LWCF, **(c)** SWCF + LWCF, **(d)** all-sky OLR, **(e)** clear-sky OLR, and **(f)** TOA radiation imbalance on CCN number concentration at 1 % supersaturation in simulations with fixed (red) and interactive (blue) SST.

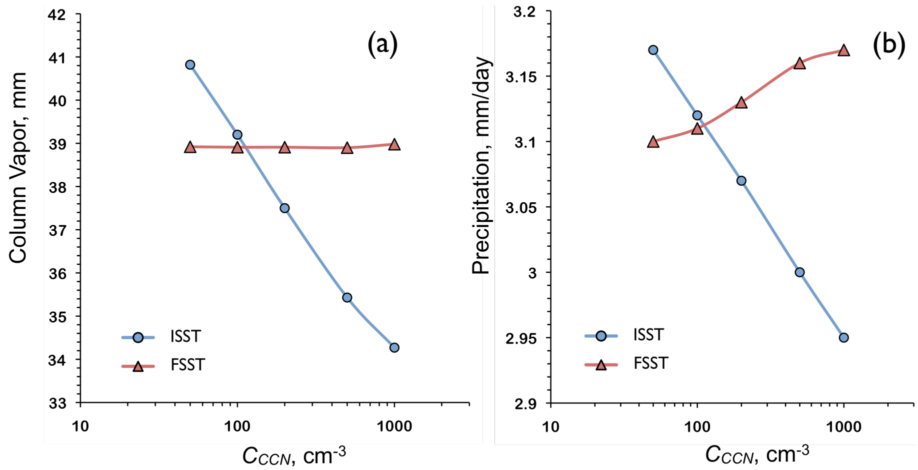

Fig. 4. Dependence of **(a)** column-integrated water vapor (precipitable water), and **(b)** surface precipitation on CCN number concentration at 1 % supersaturation in simulations with fixed (red) and interactive (blue) SST.

ACPD
12, 29099–29127, 2012

Cloud-resolving modeling of aerosol indirect effects

M. F. Khairoutdinov and C.-E. Yang

Title Page
Abstract | Introduction
Conclusions | References
Tables | Figures
◀| |▶
◀ ▶
Back | Close
Full Screen / Esc
Printer-friendly Version
Interactive Discussion

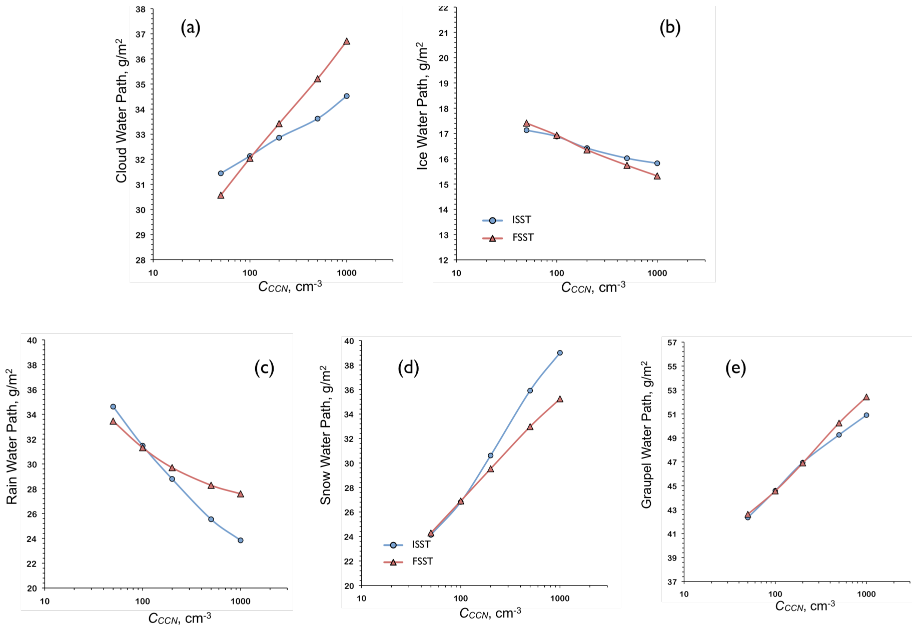

Fig. 5. Dependence of column-integrated **(a)** liquid cloud water, **(b)** cloud ice, **(c)** rain water, **(d)** snow water, and **(e)** graupel water on CCN number concentration at 1 % supersaturation in simulations with fixed (red) and interactive (blue) SSTs.

ACPD
12, 29099–29127, 2012

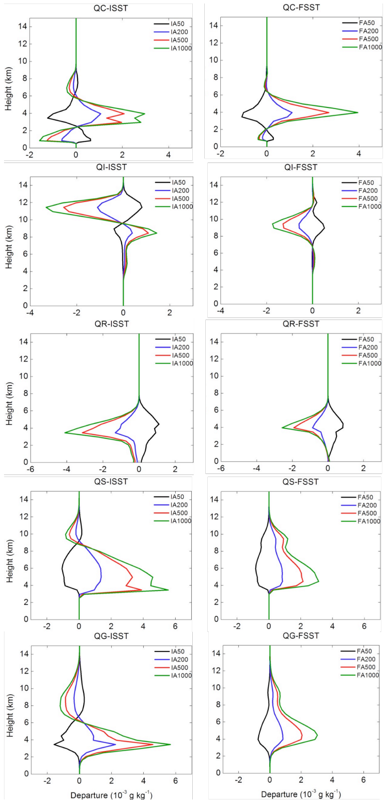

Fig. 6. Vertical profiles of departure from the control (IA100 and FA100) of the mixing ratio in $10^{-3}\,\mathrm{g\,kg^{-1}}$ of cloud liquid water (QC), rain water (QR), cloud ice (QI), snow (QS), and graupel (QG) for interactive (left panels) and fixed (right panels) SSTs.

ACPD
12, 29099–29127, 2012

Cloud-resolving modeling of aerosol indirect effects

M. F. Khairoutdinov and C.-E. Yang

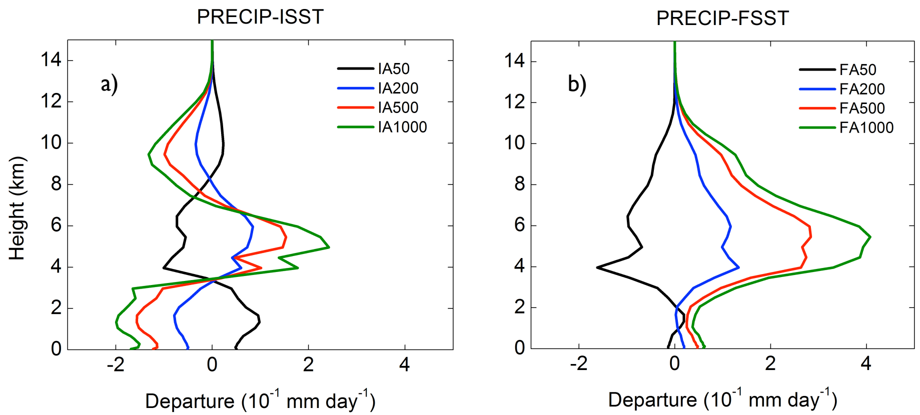

Fig. 7. Vertical profiles of the departures from the control (IA100 and FA100) of precipitation flux in 10^{-1} mm day^{-1} for **(a)** interactive and **(b)** fixed SST.